



UNIVERSITI  
TEKNOLOGI  
PETRONAS

**PETROPHYSICS OF PALEOZOIC LIMESTONE AT KINTA VALLEY**

By

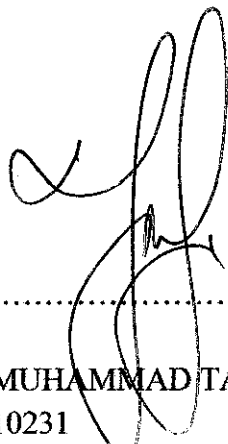
**MUHAMMAD TAUFIQ BIN YAAKOB**  
**10231**

FINAL REPORT Submission in  
Partial Fulfillment of the Requirements of the  
Bachelor of Engineering (Hons)  
Petroleum Engineering

JANUARY 2011

Universiti Teknologi PETRONAS  
Bandar Seri Iskandar  
31750 Tronoh  
Perak Darul Ridzuan.

This is to certify that I am responsible for the work submitted in this project, that the original work is my own except as specified in the references and acknowledgements, and that the original work contained herein have not been undertaken or done by unspecified sources or persons.



.....  
MUHAMMAD TAUFIQ BIN YAAKOB  
10231  
PETROLEUM ENGINEERING

**CERTIFICATION OF APPROVAL**

**PETROPHYSICS OF PALEOZOIC LIMESTONE AT KINTA VALLEY**

By

**MUHAMMAD TAUFIQ BIN YAAKOB**  
10231

A Project Dissertation Submitted to the  
Geoscience & Petroleum Programme  
Universiti Teknologi PETRONAS  
In Partial Fulfillment of the Requirements of the  
Bachelor of Engineering (Hons)  
Petroleum Engineering

Approved by,

.....  
(DR ZUHAR ZAHIR BIN TUAN HARITH)

**UNIVERSITI TEKNOLOGI PETRONAS**  
**TRONOH, PERAK**  
APRIL 2011

## **EXECUTIVE SUMMARY**

This report provides an analysis and findings throughout the entire progress towards the completion of the project: **PETROPHYSICS OF PALEOZOIC LIMESTONE AT KINTA VALLEY**. It consists of introduction of Kinta Valley limestone, problem that occurred, methodology of the project and result of the project. This project is focusing on the Paleozoic Limestone samples collected from Kinta Valley only. The studies and discussions are limited to petrophysical properties and characterization of the sample which are:

- Rock Typing
- Acoustic Velocity
- Porosity/Permeability
- Hardness/Strength

## **ACKNOWLEDGEMENT**

I would like to express the deepest appreciation to Universiti Teknologi PETRONAS (UTP), specific to Geosciences & Petroleum Engineering Department. Therefore, thanks to Assoc. Prof. Ir. Abdul Aziz Omar, the Head of Department of Geosciences & Petroleum Engineering, Ms Mazuin Bt Jasamai, Final Year Project II coordinator, for their hard work to ensure the thriving of this subject.

I owe the deepest gratitude to Dr Zuhar Zahir bin Tuan Harith, supervisor for this project, for his guidance, advice, encouragement and endless support throughout the triumphant of this project.

It is a pleasure to thank those who contribute towards the completion of project. Especially Ms Sarah from SEACARL, Mr Samsudin from GPED, and Mr Najib from GPED for providing the materials and help needed for the study. I appreciate their support.

A token of appreciation also goes to my parents, family and colleagues for their support and kindness in making this project a success.

## **TABLE OF CONTENTS**

### **CHAPTER 1:INTRODUCTION**

1.1.	Background	1
1.2.	Problem statement	1
1.3.	Objective	1
1.4.	Scope of Studies	2

### **CHAPTER 2:LITERATURE REVIEW AND/OR THEORY**

2.1.	Paleozoic Limestone at Kinta Valley	3
2.2.	Rocks Physics	3
2.3.	Limestone Reservoir	4
2.4.	Carbonate Classification	4
2.5.	Heterogeneity	4
2.6.	Mineralogy	5
2.7.	Core Sampling	5
2.8.	Acoustic Properties	6
2.9.	Permeability	6
2.10.	Porosity	7
2.11.	Carbonate Rock	7

### **CHAPTER 3:METHODOLOGY/PROJECT WORK**

3.0.	Methodology	9
3.1.	Flowchart of Process	10
3.2.	FYP1 Workflow	11
3.3.	FYP2 Workflow	12

### **CHAPTER 4: RESULTS AND DISCUSSIONS**

4.1.	Core Sample	13
4.2.	Rock Compressibility	18
4.3.	Density	19
4.4.	Porosity and Permeability	20
4.5.	Acoustic Velocity	20
4.6.	Poissons Ratio, Shear Modulus and Elastic Coefficient	21

<b>REFERENCES</b>	<b>22</b>
-------------------	-----------

### **APPENDICES**

## **LIST OF FIGURES**

### **CHAPTER 3:            METHODOLOGY**

- Figure 1                    Project Workflow**
- Figure 2                    Gantt Chart FYP 1**
- Figure 3                    Gantt Chart FYP 2**

### **CHAPTER 4:            RESULT AND DISCUSSION**

- Figure 4                    Rock Compressibility Test**

## **LIST OF TABLE**

### **CHAPTER 3:            RESULT AND DISCUSSION**

- Table 1                    Rock Compressibility Test Result**
- Table 2                    Mercury Test Result**

# CHAPTER 1

## INTRODUCTION

### 1. INTRODUCTION

#### 1.1 Background

Kinta Valley is full of isolated limestone hills that cover 1200 km<sup>2</sup> area. Most of the limestone hills around this area display a striking tower-like morphology of thick Paleozoic age limestone. Some hills are blasted to obtain the limestone which is used in the cement industry and also for road building. Other hills which have marble are treated more gently, as the marble is extracted in large chunks, to be used as decorative stone. Further on, Gunung Lang has been turned into a water recreation park. The next noticeable limestone hill is Gunung Pondok which sticks up like a top hat. It has been heavily quarried on the side that faces the road. Some of the caves are actually archaeological sites. It is believed that Kinta Valley has a very good prospect for a future. However, failing in knowing the rock characteristics may result in the wrong interpretation of Paleozoic limestone in this area. Unlike sandstone which is more homogeneous, carbonate may have complex pore systems (heterogeneous), including interparticle, intra-particle, moldic, and vuggy pore systems formation.

#### 1.2 Problem Statement

There is limited data availability about the properties and characteristics of Paleozoic Limestone at Kinta Valley. Developing robust, accurate, and practical carbonate rock physics models is a crucial step for successful geophysical applications in carbonate reservoirs.

#### 1.3 Objectives

- To determine the characteristics and petrophysical properties of Paleozoic Limestone at Kinta Valley with relation to pore type for possible correlation to other geophysical and seismic data.



#### **1.4 Scope of Study**

This project is focusing on the Paleozoic Limestone samples collected from Kinta Valley only. The studies and discussions are limited to petrophysical properties and characterization of the sample which are:

- Rock Typing
- Acoustic Velocity
- Porosity/Permeability
- Hardness/Strength

## **CHAPTER 2**

### **LITERATURE REVIEW**

#### **2. LITERATURE REVIEW**

##### **2.1 Paleozoic Limestone at Kinta Valley**

A number of isolated limestone hills, distributed over a 1200 km<sup>2</sup> area in the Kinta Valley, display a striking tower- like morphology. The limestones hills are the remnants of thick Paleozoic Limestone deposits, mainly carboniferous to Permian in age, which have been severely eroded and karstified. Layers of shale and siltstone, several hundreds of meters thick, are interbedded with or underlie the limestone. It is suggested that Paleozoic Limestone of Kinta Valley consists of marine slope deposits.

##### **2.2 Rocks Physics**

Rock Physics provides the connections between elastic properties measured at the surface of the earth, within the borehole environment or in the laboratory with the intrinsic properties of rocks, such as mineralogy, porosity, pore shapes, pore fluids, pore pressures, permeability, viscosity, stresses and overall architecture such as laminations and fractures. Rock Physics provides the understanding and theoretical tools required to optimize all imaging and characterization solutions based on elastic data.

##### **2.3 Limestone Reservoir**

Limestone reservoirs found at increasingly greater depths, with accompanying higher per well cost of production, have made the problem of determining net pay thickness of limestone reservoirs more exacting. In discussing the petrophysics of limestone, it is necessary first to classify them in a manner to portray as much as possible the essential pore characteristics of a reservoir.

## **2.4 Carbonate Classifications**

The Lucia classification (1983, 1995, 1999) is one of the most widely applied classification for carbonate reservoirs. The basis is that the pore-size distribution is related to the rock fabric, and thereby the sorting of rock into these rock types allows for better prediction of permeability and saturation. The three primary pore systems defined by Lucia were inter-particle, vuggy separated and vuggy touching. Lucia (1999) developed three petrophysical classes by grouping the carbonate samples into three rock fabric group. Class 1 consists of grain dominated packstones (fine and medium crystalline limestone and dolomite), as well as medium crystalline mud dominated dolostones. Class 3 is composed of mud-dominated limestones as well as fine crystalline mud dominated dolomites.

The newer classification method, Lonoy (Lonoy, A. 2006), however, is a refinement of the Lucia classification method as well as the Choquette and Pray model. The Lucia pore classification method was applied to the classification of approximately 3000 plug samples by A.Lonoy. He concluded that a better relationship between porosity and permeability could be obtained by subdividing the Choquette and Pray porosity classification into patchy and uniform sub classes. He also found that for the Lucia classification, separate permeability trends exist for intercrystalline and intergranular porosity systems, lumped together, under the classification 'interparticle'. The new method incorporates these observations and gives a much improved correlation. Loony also addressed the heterogeneity of the core plug sample by selection specific core samples from a much larger data set, such that the selected plugs included only one dominant pore type. This larger data set was composed of many samples with mixed pore systems. It was found that these mixed porosity samples tended to lie between the end members, but were biased toward the pore type with higher permeability.

## **2.5 Heterogeneity**

Carbonates are characterized by different types of porosity and have unimodal, bimodal and other pore size distributions, which result in wide permeability variations for the same total porosity, making difficult to predict their producibility.

## **2.6 Mineralogy**

Carbonate mineralogy is usually simple – principal minerals are calcite, dolomite, and minor clay. Secondary minerals like anhydrite, chert, and quartz are common. Accessory minerals like phosphates, glauconite, ankerite, siderite, feldspars, and clay minerals are also present depending on the environment of deposition and diagenetic history. Disseminated pyrite present in minor quantities can affect the resistivity logs and result in apparently pessimistic estimation of oil saturation. Total gamma ray logs are insufficient to estimate clay volumes because of the presence of phosphate or organic matter, which result in relatively high uranium content. Diagnostic crystal structure of the different carbonate minerals is revealed by x-ray studies: these indicate that chemical tests for magnesium, a common basis for the classification of limestones and dolostones, are insufficient to prove the existence of the mineral dolomite. High magnesium calcite occurs in many carbonates, often indicating little diagenesis. Correct mineralogy is important for accurate estimation of porosity using nuclear devices. Elemental concentration spectroscopy logs provide valuable information to address this problem. There may be a relationship between mineralogy and reservoir quality.

## **2.7 Core Sampling**

Core samples provide a valuable data source for investigating geological heterogeneity and understanding reservoir quality and performance. Many analytical techniques are employed to investigate heterogeneities at different scales, such as core description, thin section petrography and mineralogy, core plug analysis and wireline log/seismic data calibration. As an initial effort, very small scale heterogeneities are examined using thin sections and samples from slabbed cores, such as reservoir texture, fauna/flora, grain size, mineralogy, and diagenetic history. Conventional core plugs examine a large scale heterogeneity and reveal pore size distributions and reservoir quality (porosity/permeability). Core recovery and quality are of serious concerns in carbonate reservoirs. Cores from fragile formations are lost or damaged leading to depth matching issues and unreliable measurements of reservoir properties.

## **2.8 Acoustic Properties**

Acoustic is usually pertaining to sound. Generally, acoustic describes sound or vibrational events, regardless of frequency. The term sonic is limited to frequencies and tools operated in the frequency range of 1 to 25 kilohertz. In geophysics, acoustic refers specifically to P-waves in the absence of S-waves.

Acoustic log is a display of travelttime of acoustic waves versus depth in a well. The term is sometimes used to refer specifically to the sonic log, in the sense of the formation compressional slowness. However, it may also refer to any other sonic measurement, for example shear, flexural and Stoneley slownesses or amplitudes, or to ultrasonic measurements such as the borehole televiewer and other pulse-echo devices and noise logs.

Acoustic wave is a general term for P-wave. An elastic body wave or sound wave in which particles oscillate in the direction the wave propagates. P-waves are the waves studied in conventional seismic data. P-waves incident on an interface at other than normal incidence can produce reflected and transmitted S-waves, in that case known as converted waves.

## **2.9 Permeability**

Permeability is the ability or measurement of a rock's ability to transmit fluids, typically measured in darcies or milidarcies. Impermeable formations, such as shales and siltstones tend to be finer grained or of a mixed grain size, with smaller, fewer, or less interconnected pores. Absolute permeability the measurement of the permeability conducted when a single fluid or phase is present in the rock. Effective permeability is the ability to preferentially flow or transmit a particular fluid through a rock when other immiscible fluids are present in the reservoir. The relative saturations of the fluids as well as the nature of the reservoir affect the effective permeability. Relative permeability is the ratio of effective of a particular fluid at a particular saturation to absolute permeability of that fluid at total saturation. Calculation of relative permeability allows for comparison of the different abilities of fluids to flow in the presence of each other, since the presence of more than one fluid generally inhibits flow.

## **2.10 Porosity**

Many solid and powder materials both natural (stones, soils, mineral) and manufactured (catalyst, cements, pharmaceuticals, etc) contain a certain internal volume of empty space. This is distributed within the solid mass in the form of pores, cavities, and cracks of various shapes and sizes. The total sum of these void volumes is called porosity. Porosity strongly determines important physical properties of material such as durability, mechanical strength, in order to predict their behavior under different environmental conditions. There are two main and important typologies of pores: open and closed pores. Closed pores are completely isolated from the external surface, not allowing the access of external fluids in neither liquid nor gaseous phase. Closed pores influence parameters like density, mechanical and thermal properties. Open pores are connected to the external surface and are therefore accessible to fluids, depending on the pore nature/size and the nature of the fluid. Open pores can be further divided into dead-end or interconnected

## **2.11 Carbonate Rock**

Carbonate sediments have a wide range of particle size and sorting because they are formed by organic activity and redistributed by current transport. Porosity values range from 40% to 75% and permeabilities from 200 to 30,000 md. Mud-dominated fabrics average 70% porosity and 200md permeability, grain-dominated packstones average 55% porosity and 1,800md permeability, and grainstones average 45% porosity and 30,000md permeability. Pore space is located between and within depositional grains. Interparticle pore-size is a function of the particle type, size, and sorting with particle sizes ranging from 5 micron mud to large ooids and coral fragments. Intraparticle pore sizes (separate vugs) range from microporosity in ooids and peloids to relatively large intraskeletal pores.

The spatial distribution of petrophysical properties is linked to facies patterns. Rock-fabric facies are systematically distributed within high-frequency cycles and within high-frequency sequences. These are chronostratigraphic units bounded by time surfaces that can be correlated from well to well. Depositional textures are vertically stacked into tidal-flat capped cycles and subtidal cycles that may be capped by bindstone, grainstone, grain-dominated packstone, mud-dominated packstone, or wackestone depending on the depositional energy. Depositional energy is controlled by topography and the types of ocean

currents. The highest energy is generally located at the shelf margin and the cycles are typically capped by bindstone, grainstone, or grain-dominated packstone. Gentle currents are typically found over the middle shelf, except during storms, and mud-dominated cycles with thin mud- to grain-dominated packstones are cycle caps. The shoreline is a trap for sediment transported from the subtidal to the shore, forming beaches and tidal-flat-capped cycles. A variety of currents are found basinward of the shelf crest, depositing mud dominated sediment as well as graded beds and boulder beds. The two basic cycles, however, are tidal-flat capped and subtidal, and subtidal cycles are commonly composed of two basic textures, a lower mud-dominated texture and an upper grain-dominated cap.

Each HFC begins with a flooding event produced by a relative sealevel rise. Flooding events approximate chronostratigraphic surfaces and define the HFC as a time-stratigraphic unit. High-frequency cycles stacked into retrogradational cycles indicate an overall sea-level rise, aggradational cycles indicate a sea level still stand, and progradational cycles indicate a general sea-level fall. The sequence from retrogradational to progradational defines a larger sea-level signal and is referred to as a high-frequency sequence. The systematic patterns of depositional textures organized within the high-frequency sequence define the distribution of petrophysical properties at the cycle scale.

There are no nonproductive areas in the depositional model because very few sediments can be considered nonreservoir quality. However, bodies of high-permeability sediment are located in the vicinity of the shelf crest and are bounded seaward and landward by low-permeability mud-dominated sediments. Petroleum reservoirs commonly have nonproductive areas because diagenetic processes modify depositional texture, most commonly reducing porosity and permeability

.Carbonate sedimentary textures are systematically distributed on a carbonate platform. Assuming the products of diagenesis conform reasonably well to the depositional textures, predictions of petrophysical properties can be made based on predictions of the three-dimensional patterns of petrophysically significant depositional facies. Depositional patterns in carbonates are highly variable.

## **CHAPTER 3**

### **METHODOLOGY**

#### **3. METHODOLOGY**

This project consists of 3 main stages. The first stage is a research about the location and other relevant things that related to the topic. The sources of references are Society of Petroleum Engineers published papers, online references, and books that related to limestone and petrophysics.

The second stage is sample collection. The location will be based on the existing geological report of Kinta Valley to identify the area that contains Paleozoic Limestone. Then, a sample of Paleozoic Limestone are collected and prepared. For this project, the core plug of the sample taken will be made in 1" diameter, 1"-2" length. This stage needs a field trip to gather the sample.

The third stage will be the laboratory works to test the collected sample during second stage. For this stage, samples will undergo a series of laboratory test to find:

- Rock Typing
- Acoustic Velocity
- Porosity/Permeability
- Density
- Hardness/Strength

Results from these tests will be compiled and discussed. Finally, a report will be made on to compile all the results obtained.



### 3.1 Flowchart of Process

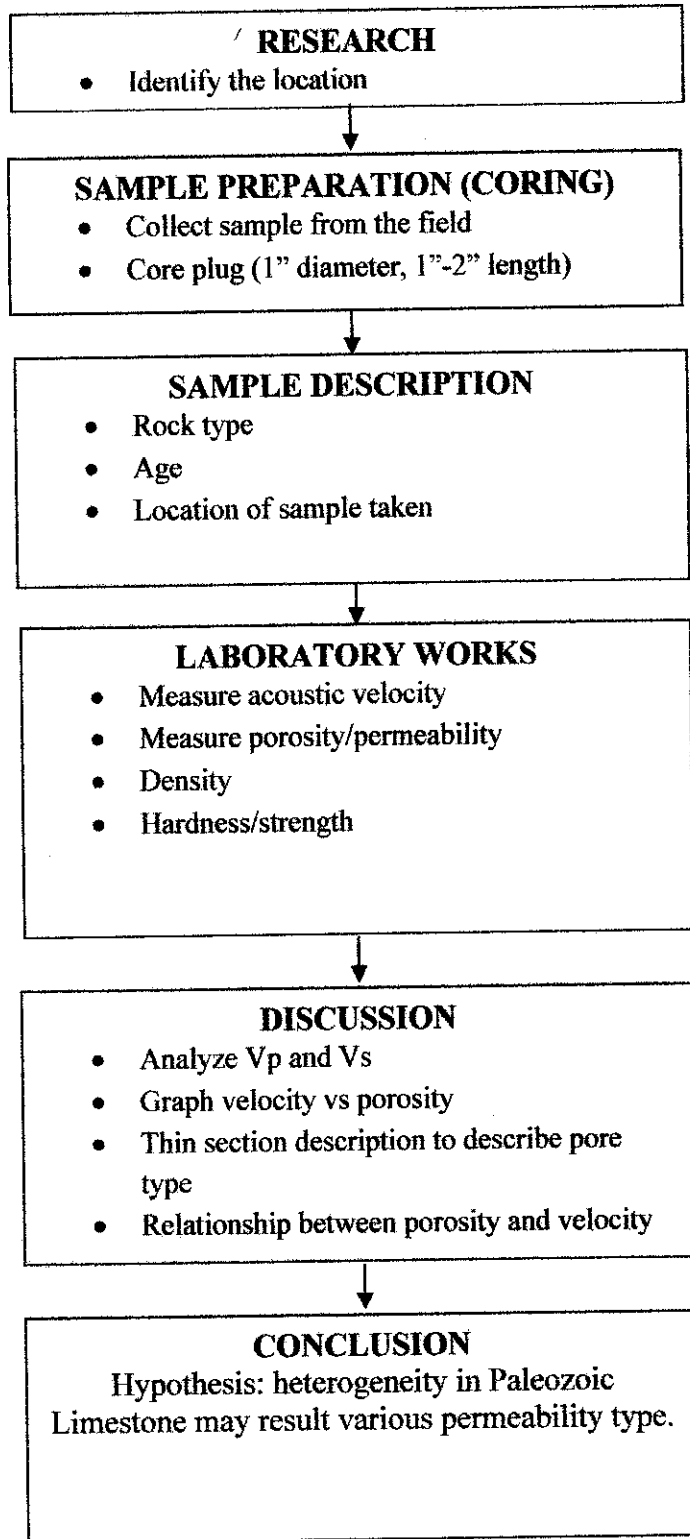


Figure 1: Process Flowchart

### 3.2 Workflow for FYP 1

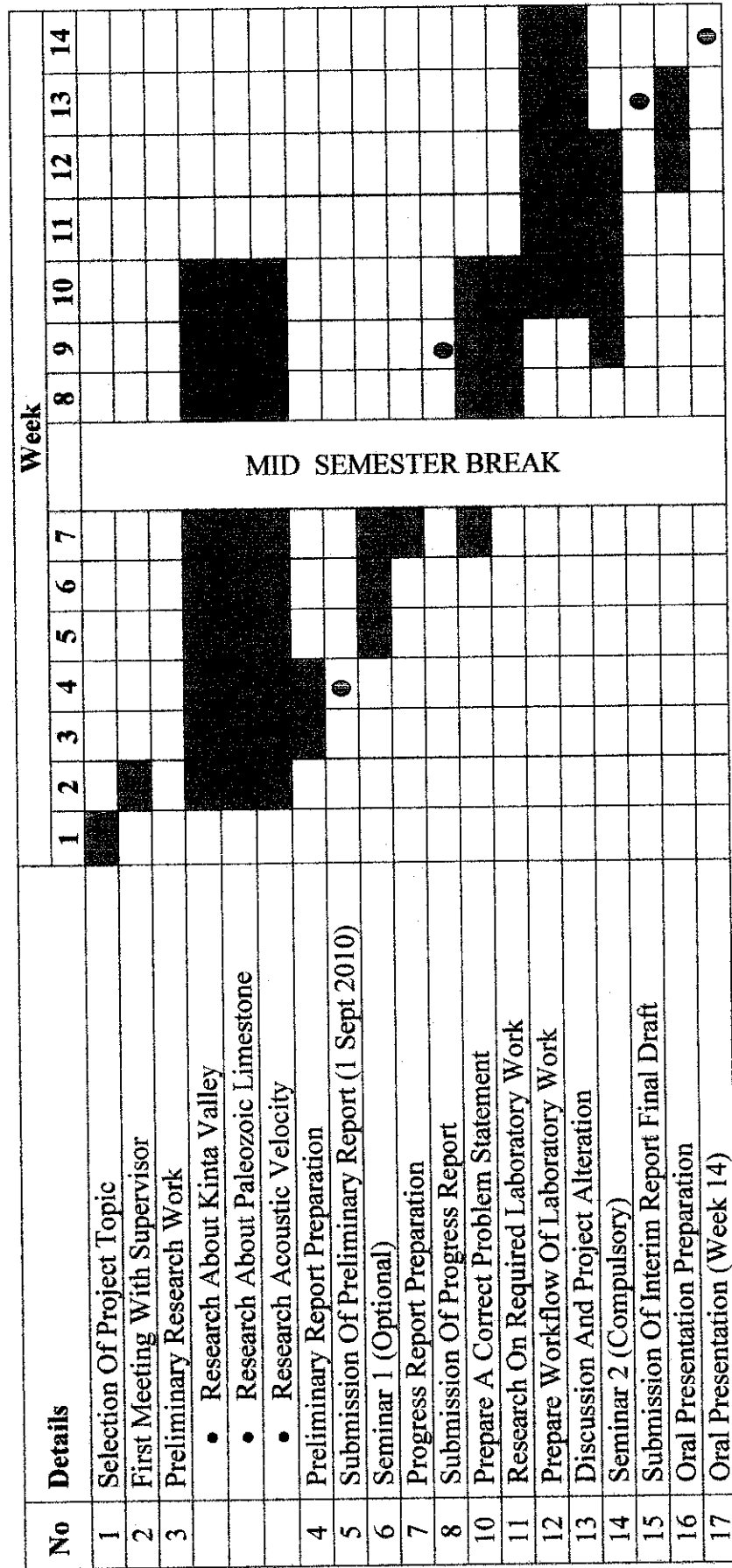


Figure 2: Gantt Chart FDP 1

### 3.2 Workflow for FYP 2

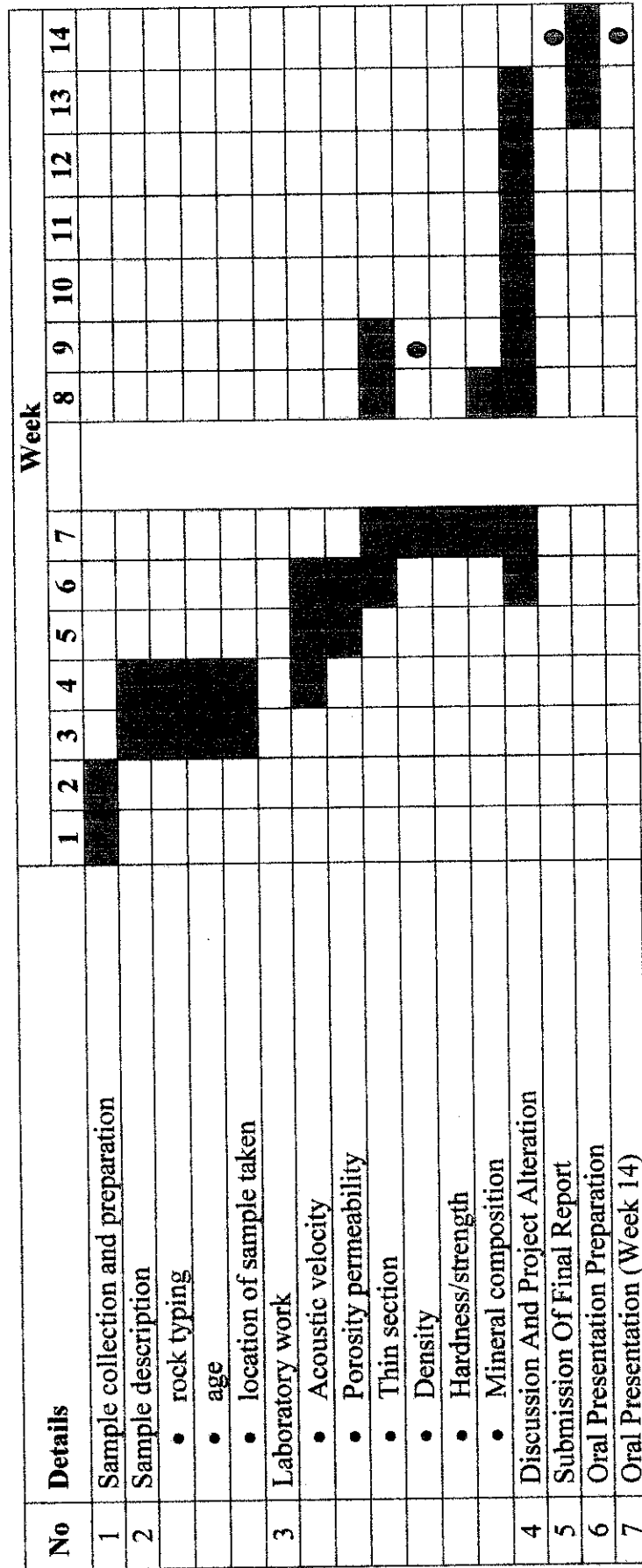
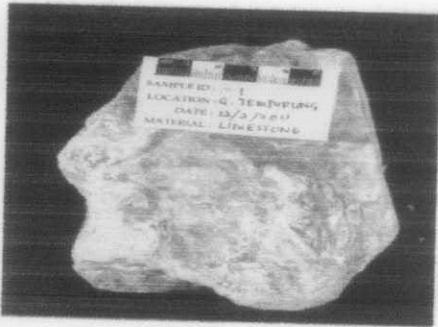



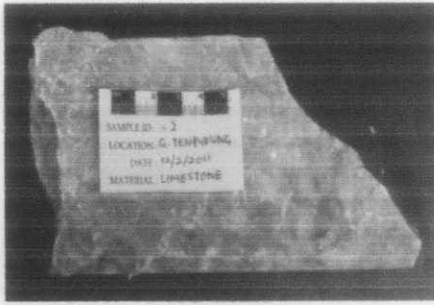
Figure 3: Gantt Chart FDP 2

**CHAPTER 3**  
**RESULTS AND DISCUSSION**

**4.1 Core Plug**

SAMPLE	CORE PLUG	DETAILS
<p><b>Sample ID: 1</b></p>  <p><b>Location:</b> Gunung Tempurung</p> <p><b>Coordinate:</b> (<math>\pm 6</math> m) N <math>04^{\circ} 25' 04.1''</math> E <math>101^{\circ} 11' 14.6''</math></p> <p><b>Material:</b> Limestone</p> <p><b>Colour:</b> White</p>		<p><b>Length:</b> 5.5 cm</p> <p><b>Weight:</b> 77.6 gm</p> <p><b>Volume:</b> 28.0924 gm<sup>3</sup></p> <p><b>Density:</b> 2.775 gm/cm<sup>3</sup></p> <p><b>Acoustic Velocity:</b> P: 2381 m/S S: 1815 m/S</p>

**Sample ID: 2**



**Location:** Gunung Tempurung

**Coordinate:** ( $\pm 6$  m)

N  $04^{\circ} 25' 04.9''$

E  $101^{\circ} 11' 15.3''$

**Material:**

Limestone

**Colour:**

Brown



**Length:**

5.1 cm

**Weight:**

72.10 gm

**Volume:**

26.049 gm<sup>3</sup>

**Density:**

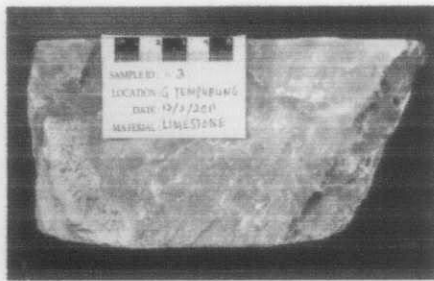
2.768 gm/cm<sup>3</sup>

**Acoustic Velocity:**

P: 4783 m/S

S: 4472 m/S

**Sample ID: 3**



**Location:** Gunung Tempurung

**Coordinate:** ( $\pm 6$  m)

N  $04^{\circ} 25' 05.2''$

E  $101^{\circ} 11' 14.0''$

**Material:**

Limestone

**Colour:**

Yellowish Brown



**Length:**

4.9 cm

**Weight:**

69.6 gm

**Volume:**

25.028 gm<sup>3</sup>

**Density:**

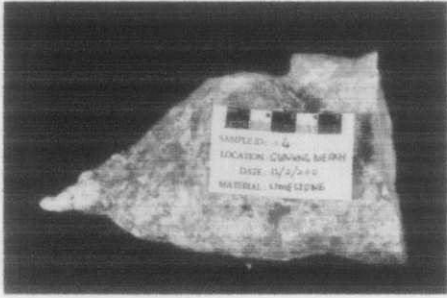
2.781 gm/cm<sup>3</sup>

**Acoustic Velocity:**

P: 5052 m/S

S: 4050 m/S

**Sample ID: 4**



**Location:** Gunung Mesah

**Coordinate:** ( $\pm 6$  m)

N  $04^{\circ} 26' 39.3''$

E  $101^{\circ} 10' 02.3''$

**Material:**  
Limestone

**Colour:**  
Yellowish Brown



**Length:**  
4.9 cm

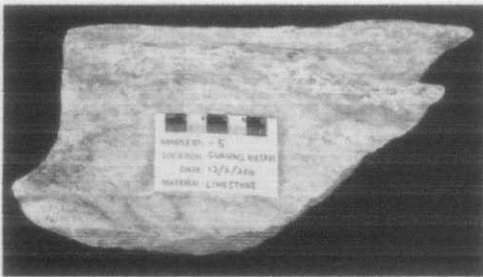
**Weight:**  
60.70gm

**Volume:**  
 $25.028 \text{ gm}^3$

**Density:**  
 $2.425 \text{ gm/cm}^3$

**Acoustic Velocity:**  
P: 4188 m/S  
S: 2832 m/S

**Sample ID: 5**



**Location:** Gunung Mesah

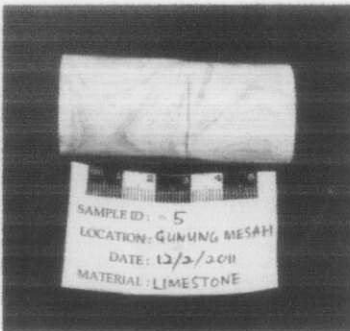
**Coordinate:** ( $\pm 6$  m)

N  $04^{\circ} 26' 39.1''$

E  $101^{\circ} 10' 01.6''$

**Material:**  
Limestone

**Colour:**  
Brown



**Length:**  
3.65 cm

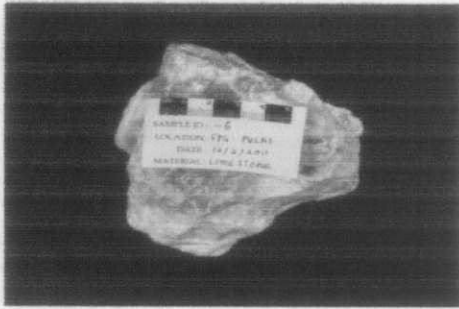
**Weight:**  
49.190 gm

**Volume:**  
 $18.643 \text{ gm}^3$

**Density:**  
 $2.639 \text{ gm/cm}^3$

**Acoustic Velocity:**  
P: 4294 m/S  
S: 7766 m/S

**Sample ID: 6**



**Location:** Simpang Pulai

**Coordinate:** ( $\pm 6$  m)

N 04° 28' 13.9"

E 101° 09' 31.8"

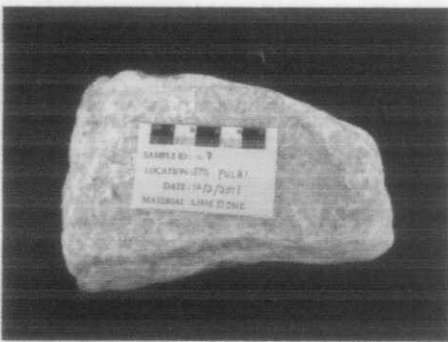
**Material:**

Limestone

**Colour:**

Brownish white

**Sample ID: 7**



**Location:** Simpang Pulai

**Coordinate:** ( $\pm 6$  m)

N 04° 25' 13.9"

E 101° 09' 31.8"

**Material:**

Limestone

**Colour:**

Brown



**Length:**

4.65 cm

**Weight:**

65.93 gm

**Volume:**

23.751 gm<sup>3</sup>

**Density:**

2.776 gm/cm<sup>3</sup>

**Acoustic Velocity:**

P: 4515 m/S

S: 5741 m/S



**Length:**

4.9 cm

**Weight:**

69.47 gm

**Volume:**

25.028 gm<sup>3</sup>

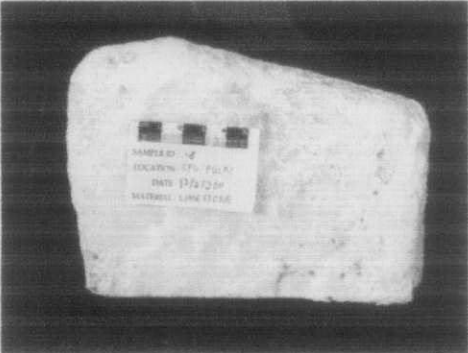

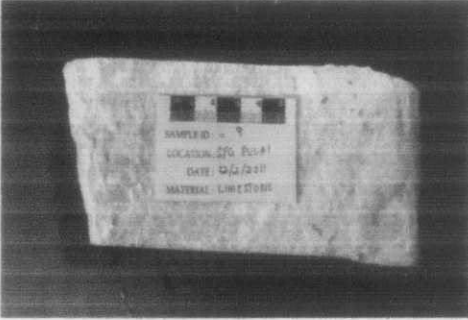

**Density:**

2.776 gm/cm<sup>3</sup>

**Acoustic Velocity:**

P: 4851 m/S

S: 8305 m/S

<p><b>Sample ID:8</b></p>  <p><b>Location:</b> Simpang Pulai</p> <p><b>Coordinate:</b> (<math>\pm 6</math> m)  N 04° 25' 13.9"  E 101° 09' 31.8"</p> <p><b>Material:</b>  Limestone</p> <p><b>Colour:</b>  Orange White</p>		<p><b>Length:</b>  5.2 cm</p> <p><b>Weight:</b>  74.11 gm</p> <p><b>Volume:</b>  26.56 gm<sup>3</sup></p> <p><b>Density:</b>  2.790 gm/cm<sup>3</sup></p> <p><b>Acoustic Velocity:</b>  P: 4860 m/S  S: 5714 m/S</p>
<p><b>Sample ID: 9</b></p>  <p><b>Location:</b> Simpang Pulai</p> <p><b>Coordinate:</b> (<math>\pm 6</math> m)  N 04° 25' 13.9"  E 101° 09' 31.8"</p> <p><b>Material:</b>  Limestone</p> <p><b>Colour:</b>  Brown</p>		<p><b>Length:</b>  5.3 cm</p> <p><b>Weight:</b>  74.67 gm</p> <p><b>Volume:</b>  27.071 gm<sup>3</sup></p> <p><b>Density:</b>  2.776 gm/cm<sup>3</sup></p> <p><b>Acoustic Velocity:</b>  P: 4953 m/S  S: 5354 m/S</p>



## 4.2 Rock Compressibility



Figure 4: Rock Compressibility Test Machine

Rock sample	Pressure Applied before break
1	1.90 KN / 1.88 MPa
2	2.24 KN / 2.21 MPa
3	2.06 KN / 2.03 MPa
4	2.82 KN / 2.79 MPa
5	2.83 Kn / 2.81 MPa
6	3.21 KN / 3.18 MPa
7	3.46 KN / 3.42 MPa
8	3.78 KN / 3.74 MPa
9	3.52 KN / 3.48 MPa

Table 1: Rock Compressibility Result

Samples are tested by applying pressure towards sample until the samples are broken. The reading is taken is the pressure that the sample can withstand before it break. The test is done by using rock compressibility test equipment. The highest pressure that sample can withstand is from sample 3.78 KN / 3.74 MPa (sample 8) while the lowest pressure that sample can withstand is 1.90 KN /1.88 MPa (sample 1)

### 4.3 Porosity and Permeability

Porosity and permeability of the sample is tested by using mercury injection. For this test, only two samples ( sample 3 and 5) are tested. The principle of the technique is based on the fact that mercury behaves as a non-wetting liquid toward most substances. This technique is not advisable when the sample contains metals reacting with mercury and forming amalgam. Mercury is forced to enter into the pores by applying a controlled increasing pressure. As the sample holder is filled with mercury under vacuum conditions (mercury surrounds the sample without entering the pores due to the very low residual pressure), during the experiment the pressure is increased and the volume of mercury in the sample holder represents the pore volume. The method is based on the capillary depressurization phenomenon. In a porous body, the surface tension forces are opposed to the penetration by liquids showing a contact angle higher more than 90° (nonwetting liquids). It is necessary to apply a pressure to mercury compensating the pressure difference over the mercury meniscus in the porous body. The result of the test is as below:

<b>SAMPLE</b>	<b>5</b>	<b>3</b>
Accessible Porosity (%)	6.92	4.12
Inaccessible Porosity (%)	-2380.2	-1202.17
Cylindrical pores permeability ( $\mu\text{m}^2$ )	557.61E-6	557.61E-6
General permeability ( $\mu\text{m}^2$ )	518.27E-6	518.27E-6

*Table 2: Porosity and Permeability Test*

#### **4.4 Density**

Density of the rock sample is calculated manually from the core plug (1 in x 2 in). From the test conducted, the density of the rock sample is ranging from 2.425 g/cm<sup>3</sup> to 2.790 g/cm<sup>3</sup>. The highest density is calculated from sample 8 (2.790 g/cm<sup>3</sup>) while the lowest density is calculated from sample 3 (2.425 g/cm<sup>3</sup>). The average density for all samples is 2.722 g/cm<sup>3</sup>.

#### **4.5 Acoustic Velocity (Ultrasonic Velocity Measuring System for Rock Sample)**

The SonicViewer-SX is an instrument for the ultrasonic wave velocity measurement of rock samples. It is possible to read the P and S wave propagation with high accuracy because it contains high voltage (500V) pulser and receiver which consists of 10 bit, 50nsec A to D converter. In addition, input of the parameter of length and density of the rock sample calculate dynamic poisson's ration and dynamic shear modulus by built in software.

For this project, the highest P-velocity is obtained from sample 3 (5052 m/S) while the lowest P-wave is obtained from sample 5 (4188 m/S). Average P-wave for all samples is 4727 m/S. For the S-velocity the highest value is obtained from sample 7 (8305 m/S) while the lowest P-wave is obtained from sample 4 (2832 m/S). Average P-wave for all samples is 5383 m/S. there might be an error while determining the time where the wave enters the sample which might effects the result. So the process is done carefully in order to get the perfect result.

#### 4.6 Poisson's Ratio, Shear Modulus, and Elastic Coefficient

SAMPLE	POISSON'S RATIO	SHEAR MODULUS	ELASTIC COEFFICIENT
1	-2.97e+000	5.55e+007	-2.19e+008 kN/m <sup>2</sup>
2	-6.49e-001	4.39e+007	3.45e+007 kN/m <sup>2</sup>
3	-3.99e-001	4.56e+007	5.48e+007 kN/m <sup>2</sup>
4	7.85e-002	1.95e+007	4.20e+007 kN/m <sup>2</sup>
5	1.22e+000	1.59e+008	7.07e+008 kN/m <sup>2</sup>
6	1.81e+000	9.15e+007	5.14e+008 kN/m <sup>2</sup>
7	1.26e+000	1.91e+008	8.65e+008 kN/m <sup>2</sup>
8	2.31e+000	9.11e+007	6.03e+008 kN/m <sup>2</sup>
9	3.97e+000	7.40e+007	7.36e+008 kN/m <sup>2</sup>

*Table 3: Poisson's ratio, shear modulus and Elastic Coefficient result*

## REFERENCES

1. G. E. Archie.1952. **Classification of Carbonate Reservoir Rocks and Petrophysical Considerations.** AAPG Bulletin
2. Askury A. Kadir, Bernard J. Pierson, Zuhar Zahir Tuan Harith, and Chow Weng Sum. 2008. **Paleozoic Limestone of the Kinta Valley: Paleogeography and Implications to the Regional and Petroleum Geology of Peninsular Malaysia.** International Petroleum Technology Conference, 3-5 December 2008, Kuala Lumpur, Malaysia
3. M.H. Mohammadlou, SPE, M.B. Mørk, and H. Langeland. 2010. **Integrated Permeability Analysis in Tight and Brecciated Carbonate Reservoir.** SPE Annual Technical Conference and Exhibition, 20-22 September 2010, Florence, Italy
4. M. I. Al-Husseini,(Saudi Aramco, Saudi Arabia). 1991. **Potential Petroleum Resources of the Paleozoic Rocks of Saudi Arabia.** 3th World Petroleum Congress, October 20 - 25, 1991 , Buenos Aires, Brazil
5. Peter A. Scholle, USGS. 1981. **Porosity Prediction in Shallow vs. Deepwater Limestones.** Journal of Petroleum Technology
6. Abdullah Sani Hashim,1991, **Kajian Penilaian Potensi Batu Kapur di Perak,** Geological Survey Department Malaysia.

## **LIST OF APPENDICES**

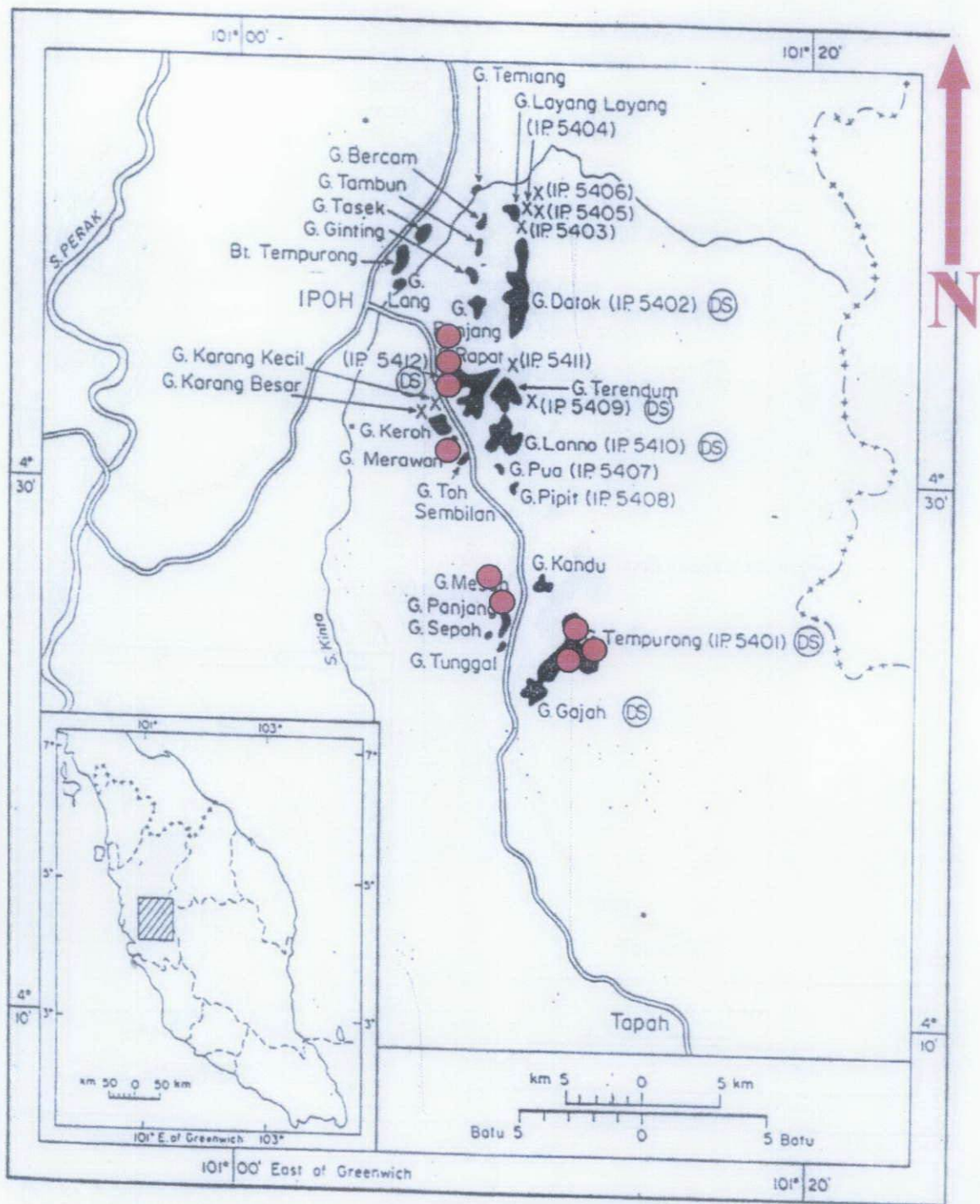
**APPENDIX 1 : Kinta Valley Map( location of sample collected)**

**APPENDIX 2 :Picture of sample taking**

**APPENDIX 3 : Acoustic Velocity Test**

**APPENDIX 4-12 : Acoustic Velocity Result**

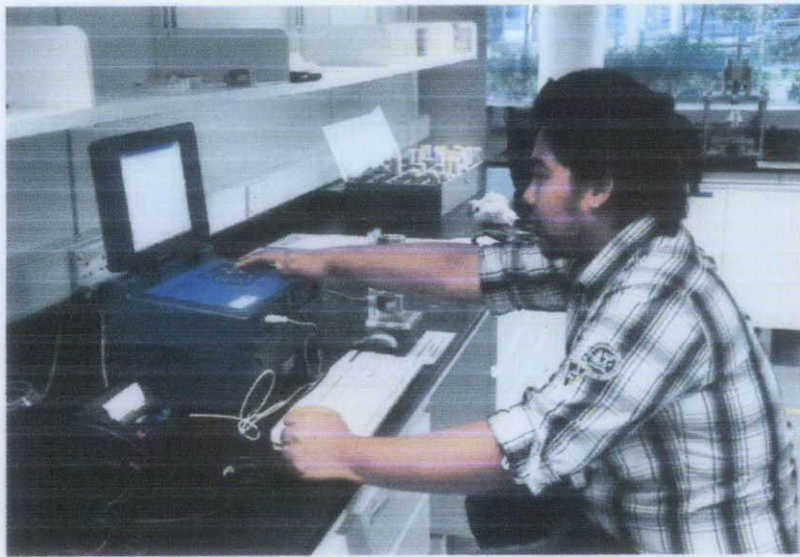
**APPENDIX 13-14 : Mercury test Result for sample 3 and 5**



appendix 1: Kinta Valley Map (location of sample collected)



*appendix 2: picture of sample taking*

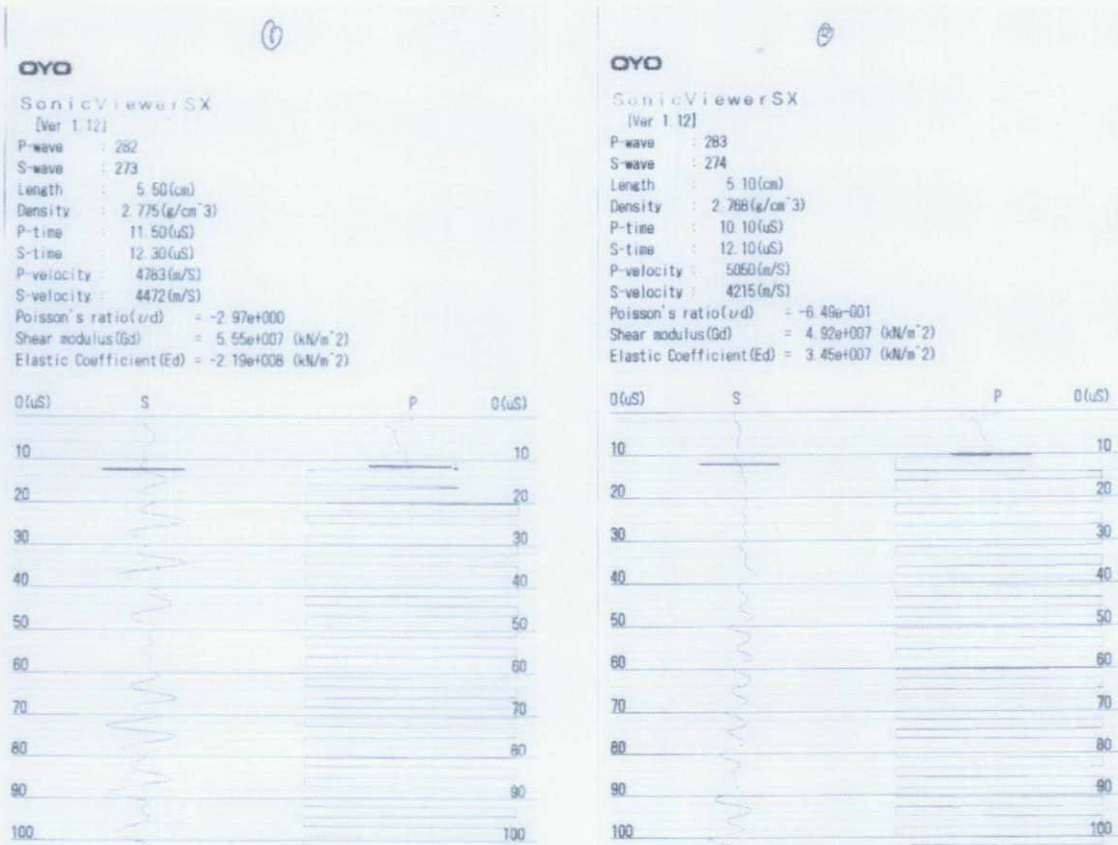


*appendix 3: acoustic velocity test*





Appendix 4: Mercury Injection Test Machine



Appendix 5-6: acoustic velocity result for sample 1 and 2

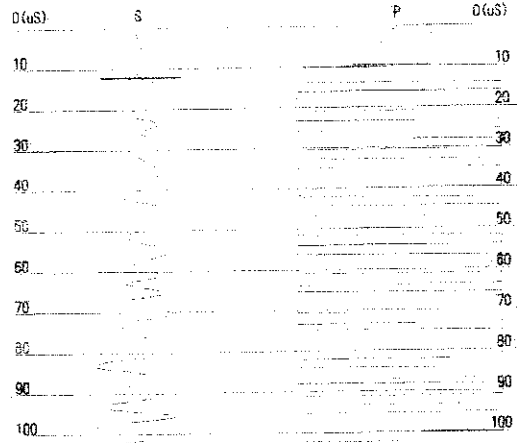
3

DYO

Sonic Viewer SX

[Ver 1.12]

P-wave : 284  
S-wave : 275  
Length : 4.90 (cm)  
Density : 2.781 (g/cm<sup>3</sup>)  
P-time : 9.70 (uS)  
S-time : 12.10 (uS)  
P-velocity : 5052 (m/S)  
S-velocity : 4050 (m/S)  
Poisson's ratio( $\nu$ ) = -3.99e-001  
Shear modulus(Gd) = 4.56e+007 (kN/m<sup>2</sup>)  
Elastic Coefficient (Ed) = 5.48e+007 (kN/m<sup>2</sup>)



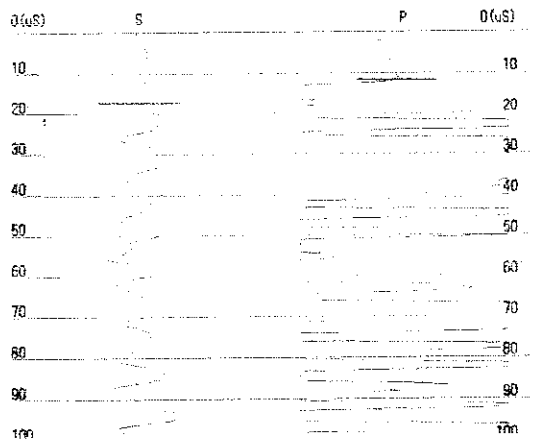
Appendix 7: acoustic velocity result for sample 3

DYO

Sonic Viewer SX

[Ver 1.12]

P wave : 285  
S wave : 276  
Length : 4.90 (cm)  
Density : 2.425 (g/cm<sup>3</sup>)  
P-time : 11.70 (uS)  
S-time : 17.30 (uS)  
P-velocity : 4188 (m/S)  
S-velocity : 2832 (m/S)  
Poisson's ratio( $\nu$ ) = 7.85e-002  
Shear modulus(Gd) = 1.95e+007 (kN/m<sup>2</sup>)  
Elastic Coefficient (Ed) = 4.20e+007 (kN/m<sup>2</sup>)



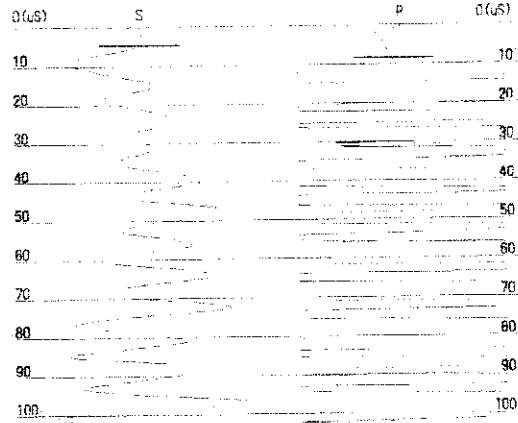
Appendix 8: acoustic velocity result for sample 4

5

OYO

Sample Viewer SX  
[Ver 1.11]

P-wave : 286  
 S-wave : 277  
 Length : 3.65(cm)  
 Density : 2.639(g/cm<sup>3</sup>)  
 P-time : 8.59(μs)  
 S-time : 4.70(μs)  
 P-velocity : 4294(m/s)  
 S-velocity : 7766(m/s)  
 Poisson's ratio(ν) = 1.22e+000  
 Shear modulus(G) = 1.69e+008 (kN/m<sup>2</sup>)  
 Elastic Coefficient(E) = 7.07e+008 (kN/m<sup>2</sup>)



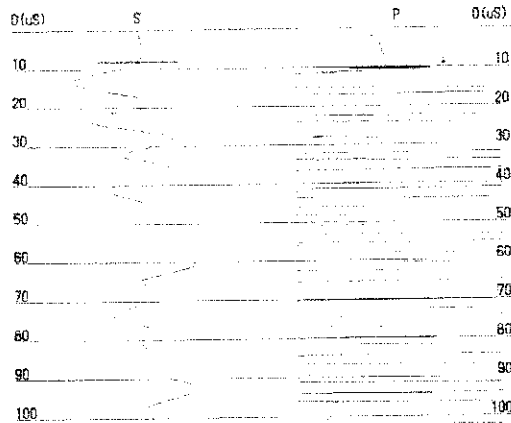
Appendix 9: acoustic velocity result for sample 5

6

OYO

Sample Viewer SX  
[Ver 1.12]

P-wave : 267  
 S-wave : 278  
 Length : 4.65(cm)  
 Density : 2.776(g/cm<sup>3</sup>)  
 P-time : 10.30(μs)  
 S-time : 8.10(μs)  
 P-velocity : 4515(m/s)  
 S-velocity : 5741(m/s)  
 Poisson's ratio(ν) = 1.81e+000  
 Shear modulus(G) = 9.15e+007 (kN/m<sup>2</sup>)  
 Elastic Coefficient(E) = 5.14e+008 (kN/m<sup>2</sup>)

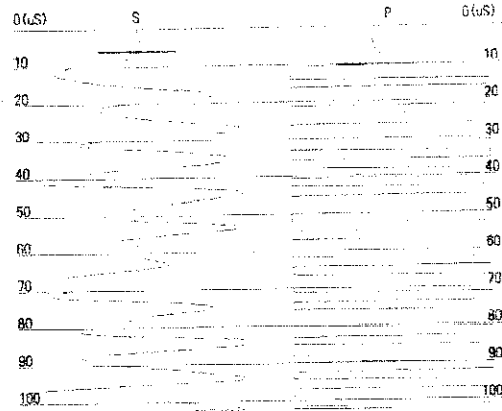


Appendix 10: acoustic velocity result for sample 6

OYO

Sonic Viewer SX  
[Ver 1.12]

P-wave : 288  
S-wave : 279  
Length : 4.90(cm)  
Density : 2.776(g/cm<sup>3</sup>)  
P-time : 10.10(μs)  
S-time : 6.90(μs)  
P-velocity : 4851(m/s)  
S-velocity : 8305(m/s)  
Poisson's ratio(ν) = 1.25e+000  
Shear modulus(G) = 1.91e+008 (kN/m<sup>2</sup>)  
Elastic Coefficient(E) = 8.05e+008 (kN/m<sup>2</sup>)



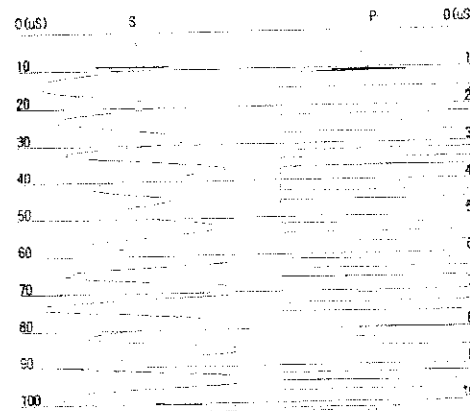
Appendix 11: acoustic velocity result for sample 7

7

OYO

Sonic Viewer SX  
[Ver 1.12]

P-wave : 289  
S-wave : 280  
Length : 5.20(cm)  
Density : 2.790(g/cm<sup>3</sup>)  
P-time : 10.70(μs)  
S-time : 9.10(μs)  
P-velocity : 4860(m/s)  
S-velocity : 5714(m/s)  
Poisson's ratio(ν) = 2.31e+000  
Shear modulus(G) = 9.11e+007 (kN/m<sup>2</sup>)  
Elastic Coefficient(E) = 6.03e+008 (kN/m<sup>2</sup>)

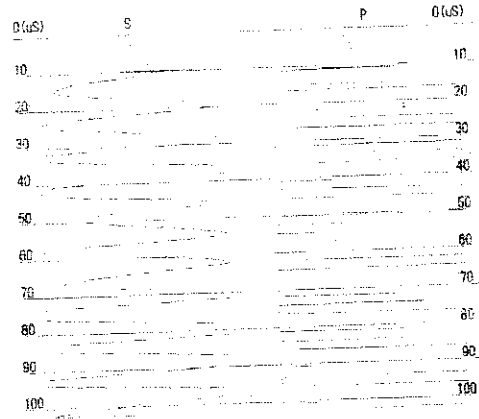


Appendix 12: acoustic velocity result for sample 8

OYO

Sample View 1 SX  
(Ver 1.12)

P-wave : 290  
S-wave : 281  
Length : 9.30(cm)  
Density : 2.851g/cm<sup>3</sup>  
P-time : 10.70(μs)  
S-time : 9(μs)  
P-velocity : 4953(m/s)  
S-velocity : 5354(m/s)  
Poisson's ratio(ν) = 0.97e+000  
Shear modulus(G) = 7.40e+007 (kN/m<sup>2</sup>)  
Elastic coefficient(E) = 7.38e+008 (kN/m<sup>2</sup>)



*Appendix 13: acoustic velocity result for sample 9*